A feasibility study quantifying in vivo human α-tocopherol metabolism[1–3]

Andrew J Clifford, Fabiana F de Moura, Charlene C Ho, Jennifer C Chuang, Jennifer Follett, James G Fadel, and Janet A Novotny

ABSTRACT

Background: Quantitation of human vitamin E metabolism is incomplete, so we quantified *RRR*- and *all-rac*-α-tocopherol metabolism in an adult.

Objective: The objective of the study was to quantify and interpret in vivo human vitamin E metabolism.

Design: A man was given an oral dose of 0.001821 μmol [5-$^{14}CH_3$]*RRR*-α-tocopheryl acetate (with 101.5 nCi ^{14}C), and its fate in plasma, plasma lipoproteins, urine, and feces was measured over time. Data were analyzed and interpreted by using kinetic modeling. The protocol was repeated later with 0.001667 μmol [5-$^{14}CH_3$]*all-rac*-α-tocopheryl acetate (with 99.98 nCi ^{14}C).

Results: *RRR*-α-tocopheryl acetate and *all-rac*-α-tocopheryl acetate were absorbed equally well (fractional absorption: ≈ 0.775). The main route of elimination was urine, and ≈90% of the absorbed dose was α-2(2′-carboxyethyl)-6-hydroxychroman. Whereas 93.8% of *RRR*-α-tocopherol flow to liver kinetic pool B from plasma was returned to plasma, only 80% of the flow of *all-rac*-α-tocopherol returned to plasma; the difference (14%) was degraded and eliminated. Thus, for newly digested α-tocopherol, the *all-rac* form is preferentially degraded and eliminated over the *RRR* form. Respective residence times in liver kinetic pool A and plasma for *RRR*-α-tocopherol were 1.16 and 2.19 times as long as those for *all-rac*-α-tocopherol. Model-estimated distributions of plasma α-tocopherol, extrahepatic tissue α-tocopherol, and liver kinetic pool B for *RRR*-α-tocopherol were, respectively, 6.77, 2.71, and 3.91 times as great as those for *all-rac*-α-tocopherol. Of the lipoproteins, HDL had the lowest ^{14}C enrichment. Liver had 2 kinetically distinct α-tocopherol pools.

Conclusions: Both isomers were well absorbed; *all-rac*-α-tocopherol was preferentially degraded and eliminated in urine, the major route. *RRR*-α-tocopherol had a longer residence time and larger distribution than did *all-rac*-α-tocopherol. Liver had 2 distinct α-tocopherol pools. The model is a hypothesis, its estimates are model-dependent, and it encourages further testing. *Am J Clin Nutr* 2006;84:1430–41.

KEY WORDS α-Tocopherol, isomer, human, metabolism, radiocarbon, accelerator mass spectrometry

INTRODUCTION

Vitamin E includes 4 tocopherols and 4 tocotrienols. Of the 4 tocopherols, α-tocopherol has the highest vitamin E activity. Natural α-tocopherol is a single stereoisomer called *RRR*-α-tocopherol. Chemically synthesized α-tocopherol is an equal mix of 8 stereoisomers and is called *all-rac*-α-tocopherol. Biologic tissues distinguish among α-tocopherol stereoisomers, and thus isomer-specific metabolism is expected (1, 2). Qualitative effects of different α-tocopherol stereoisomers are well known, but gaps exist in the understanding of the quantitative aspects of their metabolism (3–5). We aimed to quantify and interpret the metabolism of *RRR*- so as to compare it with that of *all-rac*-α-tocopherol in an adult by using kinetic modeling. Kinetic models are built and used to obtain the most complete description possible of a metabolic system under study, to obtain values for critical parameters of the model, and to identify unique and testable hypotheses about the system.

The use of radiolabeled α-tocopherol enabled the quantification of key features of the metabolism of this important vitamin (6, 7). The investigators in those studies determined that α-tocopherol was absorbed via lymph, where it peaked 2–8 h after administration. They found that it first appeared in plasma in 2–4 h, peaked there in 5–14 h, and disappeared from plasma with a $t_{1/2}$ of 53 h after administration. They found that net absorption was ≈70% and that ≈8% of α-tocopherol was eliminated via urine in 3 d. They found that almost all plasma ^{14}C radioactivity was associated with intact α-tocopherol, but that the proportion in feces was uncertain. Finally, a new derivative of administered α-tocopherol, α-tocopheryl phosphate (α-TP), was discovered in rat liver (8).

The availability of α-tocopherols selectively labeled with deuterium (d_3-, d_6-, and d_9-α-tocopherols) led to the following key discoveries. Acetate ester (ie, α-TAc), succinate ester, and free phenol forms of α-tocopherols were metabolized at the same rate (9, 10). Body α-tocopherol stores (d_0-*RRR*-α-TAc) were preferentially replaced and augmented with d_3-*RRR*-α-TAc alone

[1] From the Departments of Nutrition (AJC, FFM, CCH, JCC, and JF) and Animal Science (JGF), University of California, Davis, Davis, CA, and the Diet and Human Performance Laboratory, US Department of Agriculture, ARS, BHNRC, Beltsville, MD (JAN).

[2] Supported by grant no. DK RO1 48307, National Center for Research Resources grant no. RR13461 from the National Institutes of Health, Contract no. W-7405-Eng-48 from the US Department of Energy (to Lawrence Livermore National Laboratory), and Hoffmann LaRoche. Hoffmann-LaRoche donated the [C]α-tocopherols, and Robert Parker (Cornell University, Ithaca, NY) donated the α-CEHC reference standard.

[3] Reprints not available. Address correspondence to AJ Clifford, 3147 Meyer Hall, Department of Nutrition, University of California, Davis, One Shields Avenue, Davis, CA 95616-8669. E-mail: ajclifford@ucdavis.edu.

Received April 17, 2006.

Accepted for publication August 1, 2006.

(noncompetitive uptake protocol) over a 1:1 mix of d_6-*RRR*-α-TAc plus d_3-SRR-α-TAc (competitive uptake protocol) in replacement diets (11). It was also discovered that liver played an important role (12), that *all-rac*-α-tocopherol disappeared from plasma much faster than did *RRR*-α-tocopherol, and that this vitamin was in a state of rapid flow in and out of plasma (13). Because the absorption of α-tocopherol (as measured from plasma concentrations of deuterated and protonated α-tocopherol) was variable and low (14, 15), reassessment of that absorption for human nutritional purposes is appropriate (16).

All prior isotope studies except that of Acuff et al (17) were of relatively short duration, and thus a labeled tracer dose may not have equilibrated fully in slow-turnover α-tocopherol pools. Large doses (ie, 1700 μmol/L) relative to the Recommended Dietary Allowance (RDA) of 23 μmol/L have been used (1), and they may have influenced α-tocopherol metabolism were used. Because of biologic stereo selectivity, a true tracer-tracee relation may not have existed when an *all-rac*-α-tocopherol tracer was used for an *RRR*-α-tocopherol tracee. Therefore, we conducted a feasibility study in which we determined the fate of a true tracer dose of [^{14}C]*RRR*-α-TAc over a 63-d period; after a 3-mo washout period, we did the same for [^{14}C]*all-rac*-α-TAc in a crossover design.

SUBJECTS AND METHODS

Subject selection

The inclusion criteria stated that the subject or subjects must be 18–65 y old and healthy as determined by medical history and complete blood count and must have a body mass index (BMI; in kg/m^2) of 19–27, normal blood pressure, and a daily vitamin E intake of 7.5–12 IU/d (determined with a dietary questionnaire). Exclusion criteria were anemia; history of alcohol, drug abuse, or smoking; a serum cholesterol concentration ≥5.44 mmol/L or an LDL-cholesterol concentration >4.14 mmol/L; use of any vitamin supplement during the 3 mo before the current study; and a serum α-tocopherol concentration >24 μmol/L. Having diet supply all his α-tocopherol (*RRR*-isomer only) assured us that the [5-^{14}CH$_3$]*RRR*-α-tocopheryl acetate (TAc) served as a true tracer, and his unlabeled *RRR*-α-tocopherol served as a true tracee, even though this would not be the case with a very small dose of *all-rac*-α[5-(^{14}CH$_3$)]TAc.

Written informed consent was obtained from the volunteer under the guidelines of the Human Subjects Committee at the University of California, Davis. The study protocol was approved by that committee and by the Radiation Use Committee at the University of California, Davis. After those approvals were given, the protocol was reviewed and approved by the Lawrence Livermore National Laboratory Human Subjects Committee. The study was conducted in accordance with the ethical guidelines of the 1975 Declaration of Helsinki.

Study design

The study had a crossover design. The subject was first given an oral dose of 0.001821 μmol [5-^{14}CH$_3$]*RRR*-α-TAc (with 101.5 nCi ^{14}C), and serial samples of blood were collected for 63 d, of feces for 6 d, and of urine for 8 d after dosing. Three months from the date of [5-^{14}CH$_3$]*RRR*-α-TAc administration, the same subject was given an oral dose of 0.001667 μmol [5-^{14}CH$_3$]*all-rac*-α-TAc (with 99.98 nCi ^{14}C), and serial samples of blood were again collected for 63 d, of feces for 7 d, and of urine for 8 d after dosing.

Meals were controlled for time and content on the days that each radiolabeled tocopherol was administered. Lunch was served 5 h after dosing and consisted of a frozen chicken dinner (Lean Cuisine; Nestle USA, Wilkes-Barre, PA), salad mix, and a banana; the meal had a total fat content of ≈10 g. The following snacks were consumed between lunch and dinner: chocolate chip granola bar (Quaker; Pepsico Beverages & Foods, Chicago, IL), fat-free chocolate pudding (Jell-O; Kraft Foods Global Inc, Glenview, IL), and cranberry juice (Old Orchard Brands, LLC, Sparta, MI); the total fat content of the snacks was ≈10.5 g. Dinner was served 12.1 h after the dose and consisted of a frozen chicken enchilada dinner (Healthy Choice; ConAgra Foods Inc, Omaha, NE), baby arugula blend salad (Portofino salad; Ready Pac Produce Inc, Irwindale, CA), 5 mL (1 tsp) Italian dressing (Wish-Bone "just2good"; Unilever US Inc, Englewood Cliffs, NJ), and 226.8 g (8 oz) pine-orange juice (Dole Food Company Inc, Chicago, IL); the total fat content was ≈12 g.

Test materials

The chemical and isotopic purity of *RRR*-α[5-(^{14}CH$_3$)]-TAc (56 Ci/mol) and *all-rac*-α[5-(^{14}CH$_3$)]-TAc (60 Ci/mol) were confirmed by reisolation on HPLC and analysis on a liquid scintillation counter. Ice-cold argon-degassed ethanol was prepared by bubbling argon through 50 mL ethanol (100%) for 15 min at ≈2 °C. Each radiolabeled tocopherol was taken up (dissolved) in ice-cold argon-degassed ethanol, transferred to an amber screw-cap vial, covered with argon, and re-isolated on an Agilent 1100 HPLC with an Agilent C18 XDB column, with a 3.0 × 150–mm stationary phase (Agilent Technologies, Avondale, PA) and a 95% degassed ethanol and 5% water mobile phase pumped at 0.35 mL/min. The eluent corresponding to vitamin E was collected, fortified with sodium ascorbate (final concentration: 50 mmol/L), degassed with argon for 10 min (to minimize oxidation), and stored at −70 °C. HPLC chromatograms of the materials just before dosing showed only a single peak of ^{14}C that coeluted with α-tocopherol, which indicated that the materials did not deteriorate during storage at −70 °C in argon-degassed ethanol containing 50 mmol ascorbate/L. Finally, the 2,7,8-trimethyl-2-(2-carboxyethyl)-6-hydroxychroman (α-CEHC) reference standard was used.

Dose administration

Aliquots of the HPLC eluent with ≈100 nCi of ^{14}C were added to a cup containing a whipped mix of 10.5 g olive oil and 30 g skim milk that supplied 4.5 μmol α-tocopherol. In the case of the [5-^{14}CH$_3$]*RRR*-α-TAc, 140 μL eluent delivered 0.001821 μmol with 101.5 nCi ^{14}C. In the case of the [5-^{14}CH$_3$]*all-rac*-α-TAc, 260 μL eluent delivered 0.001667 μmol with 99.98 nCi ^{14}C. Direct addition of eluent to the whipped mixture was chosen to avoid the oxidation of the dose that might occur if it were dried and resolubilized. The subject ingested the mixture, and the cup was rinsed twice with 60 g skim milk, which the subject also ingested immediately. Dosing was conducted under observation to ensure that the entire dose was consumed. Total fat intake on the day of dosing was 32.5 g (10 + 12 + 10.5 g). Administration of an ≈100-nCi dose of radiolabeled α-tocopherol to a healthy person was feasible because accelerator mass spectrometry

(AMS) quantifies labeled biochemicals to attomolar (10^{-18}) levels in milligram-sized samples, and, at this sensitivity, the radiation exposure is similar to that from a 1-h flight in a jet, which is a level that enables in vivo testing in normal persons.

Specimen collection

Blood was drawn (glass tubes containing EDTA) on the 12th and 6th days before each dosing to ensure that the subject's plasma vitamin E status was in a steady state. Fifteen minutes before each radiolabeled tocopheryl acetate was administered, the subject was fitted with an intravenous catheter in a forearm vein, and a baseline blood sample was drawn into a 10-mL tube that contained potassium EDTA (final concentration: 1.5 mg/mL). The dose was administered and additional blood was drawn every 30 min from 0 to 12 h, every 60 min from 12 to 16 h, and then at 18, 20, 22, 24, 28, 32, 36, 40, 44, 48, 60, 72, 84, 96, 108, 120, 132, 144, 156, 168, 216, 288, 336, 504, 672, 850, and 1512 h after dosing. The catheter was removed after the 48-h blood draw. After the first and second days since dosing, blood draws were taken in the fasting state.

Urine was collected in 4-L PolyPac containers (Fisher Scientific, Fairlawn, NJ) and the weight was recorded. Urine (24-h) was collected just before the administration of each radiolabeled tocopherol to serve as the baseline value. Urine was also collected from 0 to 8 h and from 8 to 24 h after dosing. All remaining collections were 24-h collections. A 40-mL aliquot of each collection was stored at −80 °C until they were analyzed.

Feces were collected in 4-mm-thick Stomacher bags (Fisher Scientific, Fairlawn, NJ), and the weight was recorded. The subject provided a feces collection on the day before the administration of each radiolabeled tocopherol; these samples served as the baseline values. All feces for the week after dosing were collected and weighed individually.

Specimen processing

Plasma was separated from whole blood by centrifugation for 10 min at 3300 rpm and 23 °C (Fisher Scientific Model 228; Fisher Scientific, Fairlawn, NJ) and stored at −80 °C until analysis. The plasma was later analyzed for total α-tocopherol (18) to model the tracee.

Apportioning plasma ^{14}C to α-tocopherol and 2,7,8-trimethyl-2-(2-carboxyethyl)-6-hydroxychroman

Plasma (500 μL) drawn 18 h after dosing was incubated with glucuronidase, extracted with a 1:1 mix of hexane:dichloromethane containing 0.1% butylated hydroxytoluene, dried, and resuspended in ethanol as previously described (19). We used a modification of previously published HPLC conditions (19) to separate α-CEHC and α-tocopherol in a single HPLC run on a 15-μL aliquot of the ethanol extract to apportion the ^{14}C as α-CEHC and α-tocopherol. Therefore, we spiked an aliquot (15 μL) of the incubated mix with α-CEHC and α-tocopherol standards to raise their concentrations and used the following HPLC conditions: a Zorbax Bonus RP, 5 μm, 2.1 × 150–mm stationary phase (Agilent, HP), a 1:1 H_2O (pH 3.6):acetonitrile mobile phase for 0 to 6 min that was switched to a 5:95 H_2O (pH 3.6):acetonitrile for the remainder of our 20-min separation, and a flow rate of 0.4 mL/min. One-minute fractions were collected and analyzed for ^{14}C by using AMS (20, 21).

Plasma lipoproteins were isolated by using a model RC-120 GX centrifuge, an AT2 rotor, and 2-mL polyallomer reseal tubes (all: Sorvall, Newton, CT). Three solutions were prepared: solution 1 was 0.195 mol NaCl/L for density = 1.006, solution 2 was 0.195 mol NaCl/2.44 mol NaBr/L for density = 1.063, and solution 3 was 0.195 mol NaCl/6 mol NaBr/L for density = 1.26. Solution 1 (600 μL) was added to the reseal tube, underlaid with plasma (1.2 mL), and centrifuged for 23 min at 120 000 rpm and 8 °C (in the Sorvall centrifuge). Chylomicra (from the top down to 2 mm from bottom of the tube) were aspirated into a fine-tip pipette (SAMCO Scientific Corporation, San Fernando, CA) and stored in Eppendorf tubes at 4 °C. The reseal tube was sliced (2.5 mm from the bottom), and the top was discarded to avoid contamination of the denser lipoproteins with chylomicra. The bottom portion, containing the denser lipoproteins, was injected beneath a 550-μL volume of solution 1 in a new reseal tube. The new reseal tube was topped off to its original volume (as needed) with solution 1 and centrifuged for 83 min at 120 000 rpm and 8 °C to float VLDL, which was then removed as described above for chylomicra. The procedure was repeated with solution 2, which was centrifuged for 125 min at 120 000 rpm and 8 °C to float LDL that was then removed, and then with solution 3, which was centrifuged for 210 min at 120 000 rpm and 8 °C to float HDL, that was then removed. The content in the remainder of this sliced reseal tube was saved as infranatant solution.

Isolated lipoprotein fractions were extracted by adding ≈200 μL CH_2Cl_2 containing 0.01% BHT to each fraction stored in an Eppendorf tube. The sample was mixed by vortex for 1 min and centrifuged at 5000 × *g* for 5 min at 23 °C (Fisher Scientific AccuSpin Micro, NJ), and the organic layer was transferred to a new Eppendorf tube. The extraction procedure was repeated twice, by using ≈100 μL CH_2Cl_2 (containing BHT) each time, to ensure that all lipid-soluble compounds were recovered. The CH_2Cl_2 was then evaporated under argon. The residue was resuspended in 100 μL CH_2Cl_2 (containing BHT), mixed by vortex for 1 min, and centrifuged at 5000 × *g* for 5 min at 23 °C, and a 20-μL aliquot was dried at 23 °C to be used in AMS.

Urine from the third collection (24- to 48-h period after dosing with each radiolabeled α-TAc) was treated with glucoronidase and subjected to HPLC analysis (22), in which the eluent was collected in 500-μL fractions and analyzed for ^{14}C by using AMS; coelution of the ^{14}C peak with authentic α-CEHC identified the radiolabeled material in urine as [^{14}C]α-CEHC. Aliquots of urine from the fourth collection (48- to 60-h period after dosing with *all-rac*-α-[5-($^{14}CH_3$)]TAc) before and after they were treated with glucuronidase were also subjected to HPLC (22), in which the eluent was collected in 500-μL fractions and analyzed for ^{14}C by using AMS; the appearance of a ^{14}C peak only in the glucuronidase-treated sample identified the chemical nature of the ^{14}C-labeled material in urine as [^{14}C]α-CEHC-glucuronide.

Each feces collection was diluted with 5 volumes of a 50/50 solution of 1 mol potassium hydroxide/isopropyl alcohol (KOH/IPA)/L, and the mix was dispersed by using a Stomacher laboratory blender (model 3500; Fisher Scientific) for 2 min at the high setting. The sealed bag was then heated for 2 h in an 80 °C water bath. After this treatment, samples were dispersed for a second time for 2 min. The samples were returned to the 80 °C water bath for another 2 h and again dispersed for 2 min by using the Stomacher. A 40-mL aliquot was then transferred to a 50-mL centrifuge tube (Falcon conical centrifuge tube; BD Biosciences, San Jose, CA) that contained ≈8 mL glass beads (6 mm; Fisher

Scientific) and shaken (bead beaten) on a Wrist-action Shaker (model 75; Burrell Scientific, Pittsburgh, PA) for ≥4 h.

^{14}C Analysis by accelerator mass spectrometry

The neat plasma (25 μL), the HPLC fractions of the spiked 15-μL plasma extract (1-min fractions), and the isolated lipoprotein fractions (25 μL) were analyzed for ^{14}C (20, 21). Urine (100 μL) was diluted 1:10 with HPLC-grade H_2O. A 100-μL aliquot of the bead-beaten feces material was diluted 1:10 with the 50/50 KOH/IPA solution. Fifty μL of a diluted solution of tributryin in methanol (39 μL tributyrin added to 961 μL methanol) was added to all samples to ensure that each sample had 1 mg total carbon, the optimum for high quality graphite. Carbon in the samples was converted to graphite (20, 21). ^{14}C was measured at the Center for Accelerator Mass Spectrometry, Lawrence Livermore National Laboratory (Livermore, CA).

Calculations, data analysis, and presentation

The plasma data were expressed as the fraction of dose per liter of plasma and plotted as a function of elapsed time since the administration of each ^{14}C-labeled stereoisomer. The use of this fraction also enabled the ratio of plasma ^{14}C from dosed [^{14}C]*RRR*-α-TAc to that from dosed [^{14}C]*all-rac*-α-TAc to be plotted by time since dosing.

The elimination of ^{14}C via feces and urine was presented as the fraction of dose per collection, and cumulative elimination was presented as elapsed time since dose. An aliquot of the third urine collection (after each labeled isomer was administered) was treated with glucuronidase and analyzed by HPLC (22), in which 20-s fractions of eluent were collected and analyzed for ^{14}C by using AMS (21, 23) to identify and quantify [^{14}C]α-CEHC, the major urinary metabolite of the administered [^{14}C]α-tocopherols. An aliquot of the fourth urine collection (after each labeled isomer was administered) before and after treatment with glucuronidase was also analyzed by using HPLC and AMS to validate our HPLC-AMS protocol.

Kinetic modeling began with organization of the biology and metabolism of *RRR*-α-tocopherol (13, 24–32) into a model suitable for quantitative hypothesis testing. The initial model included kinetic pools for *RRR*-α-tocopherol in the gastrointestine, plasma, tissues, feces, and urine. Literature on the biology and metabolism of *RRR*-α-tocopherol suggested several possible pathways of disposition (24–32), and these were first tested individually by using rate constants initially estimated from that literature. By comparing model-estimated and observed data sets for plasma, urine, and feces, we modified the model structure and parameter values in biologically relevant ways to optimize agreement of model-estimated with observed data sets by using WinSAAM kinetic analysis software [version 3.0.7; Internet: http://www.winsaam.com (33, 34)]. Tracer and tracee patterns were used for parameter estimates, and pathways between pools were assumed to be first order. Nomenclature for the kinetic model included rate constants in which $k(i,j)$ was the daily rate to pool i from pool j, a delay in which $d(i,j)$ was the delay to pool i from pool j (in d), and flows in which $f(i,j)$ was the flow to pool i from pool j (in μmol/d). Mean residence time (in d) was calculated by dividing the number 1 by the sum of the rate constants (reciprocal), leaving a particular donor compartment of interest.

A colon pool was added to provide a slight delay during which α-tocopherol in bile (delivered to the intestine but not reabsorbed) could transit to feces. On the basis of reports in the scientific literature (2, 19, 35–39), we set 3 parameters for the model: the delay [d (to gastrointestine, from diet)] at 0.08 d; the absorption efficiency at 77.5%; and the renal clearance of α-CEHC at 50 d^{-1} [(urine α-CEHC × urine volume/d (2160 nmol/d))/(plasma α-CEHC (12 nmol/L) times plasma volume (3.58 L))]. The 3 parameters were incorporated into the WINSAAM software program. All model parameters were then optimized by using WINSAAM's least-squares routine to minimize the difference between the model prediction and experimental data.

Once the model structure and parameter values provided good visual fits, the fits were optimized by using least-squares procedures. The rate constants and distributions of α-tocopherol among the various kinetically distinguishable pools were estimated. The steady-state rate constants were estimated from the plasma patterns of the ^{14}C tracer by time since dose. Using these rate constants as we worked through the system (alternating between calculations for flows and masses), we measured the steady-state tracee masses (distributions) and in turn used them to compute tracee flows for the case of a constant daily α-tocopherol intake—ie, 12, 15, and 35 μmol/d—that corresponded to low, intermediate, and RDA (40) for vitamin E. Finally, we compared the intakes of *RRR*-α-tocopherol and *all-rac*-α-tocopherol that were needed to sustain a steady-state plasma α-tocopherol concentration of 24 μmol/L.

We first modeled the data set from administered *RRR*-α-TAc alone to determine the parameters specific to this isomer to establish a true tracer-tracee relation in the *RRR* model development. Then, using the parameters established from the *RRR* model, we compared model prediction to experimental observation for the *all-rac*-α-TAc data set. We then unlinked pathways one-by-one according to the minimal principle, unlinking the fewest rate parameters to achieve good model fits to the experimental data (41). Because the *RRR*-α-TAc parameter set maintained the values determined from the initial fitting, the linked *all-rac*-α-TAc parameters matched the corresponding *RRR*-α-TAc parameters, and the unlinked *all-rac*-α-TAc parameters were used to improve the fitting of model prediction to the *all-rac*-α-TAc data set. The *all-rac* parameters identified for unlinking were chosen on the basis of visual observation of the *all-rac* model that was fitted to observed data and of previously published observations of α-tocopherol behavior both in vitro and in vivo.

Finally, in constructing the final model, we tested the hypothesis (among others) that 2 functionally distinct pools of α-tocopherol exist in liver, liver kinetic pool A (liver A) and liver kinetic pool B (liver B) (H_o = 1 pool against the alternate hypothesis, $H_a \neq 1$ pool). Other testable hypotheses we focused on were that *RRR*- and *all-rac*-α-tocopherol shared equal rate constants for transfer to extrahepatic tissues from plasma and vice versa, for transfer to plasma from liver B and vice versa, and for catabolism to α-CEHC.

RESULTS

The subject was a 36-year-old healthy man weighing 79.5 kg and 183 cm tall. His fasting plasma chemistries were 4.55 mmol total cholesterol/L, 1.19 mmol HDL/L, 3.05 mmol LDL/L, 0.70 mmol triacylglycerol/L, ratio of total to HDL cholesterol (total:HDL cholesterol; in mg/mg) 3.8, and 30.4 μmol α-tocopherol/L. During the 2-wk period immediately before each dose

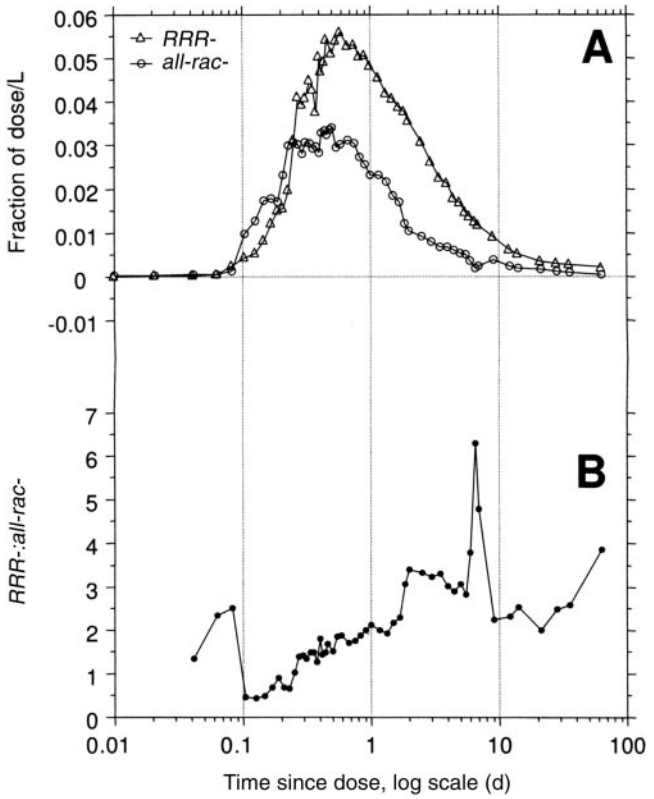

FIGURE 1. A: Pattern of ^{14}C in plasma by time since the administration of an oral dose of 0.001821 μmol [5-$^{14}CH_3$]*RRR*-α-tocopheryl acetate (with 101.5 nCi ^{14}C) and 0.001667 μmol [5-$^{14}CH_3$]*all-rac*-α-tocopheryl acetate (with 99.98 nCi ^{14}C). Doses were given to the same subject with a 3-mo intervening washout period. B: The ratio of [^{14}C]*RRR* and [^{14}C]*all-rac* in plasma after the second such dose.

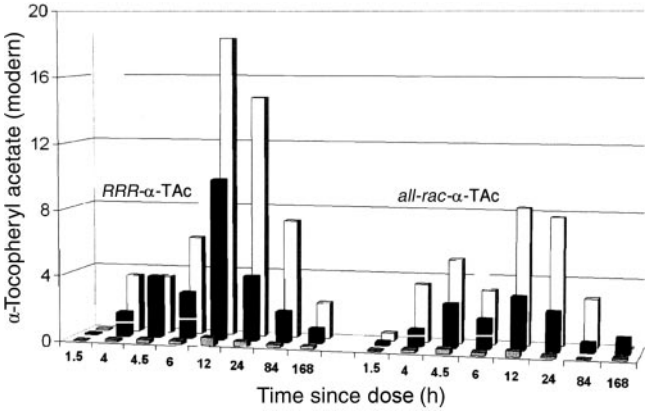

FIGURE 2. Pattern of ^{14}C in plasma lipoproteins from [^{14}C]*RRR*-α-tocopheryl acetate (TAc) and [^{14}C]*all-rac*-α-TAc. Plasma was centrifuged to separate HDL ▨, LDL □, and VLDL + chylomicron ■. Chylomicron was separated from VLDL (white stripe across the black bar, VLDL sits atop chylomicra) only at 4 and 6 h after dose for both isomers. One modern = 97.94 amol ^{14}C/mg C.

administration, the subject maintained his usual dietary habits but consumed a diet that provided only 12 ± 4 μmol *RRR*-α-tocopherol/d, which stabilized his plasma α-tocopherol at ≤23.3 μmol/L, below the threshold (30 μmol α-tocopherol/L plasma) for α-CEHC transfer into urine (42). His plasma α-tocopherol was 22.9 ± 1.0 μmol/L when he was given each radiolabeled α-tocopherol. Normal plasma concentrations are 11–37 μmol/L (43), and thus this subject was considered a healthy study subject. His plasma α-tocopherol was 22.6 μmol/L 6 d before dosing and 23.3 μmol/L 6 d after the first dose ([^{14}C]*RRR*-α-TAc), so he was in steady state with respect to his vitamin E status.

The ^{14}C tracer profiles in plasma from the administered [^{14}C]*RRR*-α-TAc and [^{14}C]*all-rac*-α-TAc in a crossover design with a 3-mo intervening washout period are shown in **Figure 1**A. The ^{14}C tracer first appeared after a delay of ≈2 h (0.08 d), peaked in 0.6 d when the ^{14}C concentration was 1.86 times that from *RRR*-α-TAc compared with *all-rac*-α-TAc, and then it returned to baseline. The 0.08-d delay represented the time needed for the oral doses to pass through the stomach and enter the duodenum, where it undergoes a phase transition from α-tocopherol in olive oil to α-tocopherol in 2-monoglyceride micelles that entered enterocytes for final transport. Figure 1B shows that the plasma ^{14}C tracer ratio (*RRR*/*all-rac*) increased from ≈0.5 at day 0.1 to 3.5 at day 2 after dosing. The ^{14}C analyte in plasma was [^{14}C]α-tocopherol, because we did not detect [^{14}C]-α-CEHC (data not shown).

The distribution of ^{14}C among plasma lipoproteins at selected times since dosing is shown in **Figure 2**. Chylomicra were separated (from VLDL) from blood drawn at 4 and 6 h only. For purposes of presentation, VLDL was stacked atop the chylomicra (so that the height above and below the white stripe = VLDL:chylomicra). In general, chylomicra and VLDL labeling with ^{14}C were similar for both isomers. The VLDL:chylomicra tended to be smaller at 4 h than at 6 h. The largest effects between the isomers occurred after 12 h, when lipoprotein labeling from administered [^{14}C]*RRR*-α-TAc was greater than that from administered [^{14}C]*all-rac*-α-TAc. The profile of labeled lipoproteins matched that of the plasma shown in Figure 1. LDL cholesterol seemed to be the major carrier of the ^{14}C, and VLDL + chylomicra ranking next; HDL appeared to be a minor carrier.

The elimination of the ^{14}C tracer in feces with the fraction of dose per collection shown in the insert is summarized in **Figure 3**. Approximately 22.5% of each administered ^{14}C tracer dose was recovered in the first 3 collections after dosing, and therefore the observed fractional absorption of the tracer for each isomer was ≈ 0.775 (range: 1.000−0.225). The model estimated fractional absorption or true digestibility [f(3,1) − [f(5,25) −

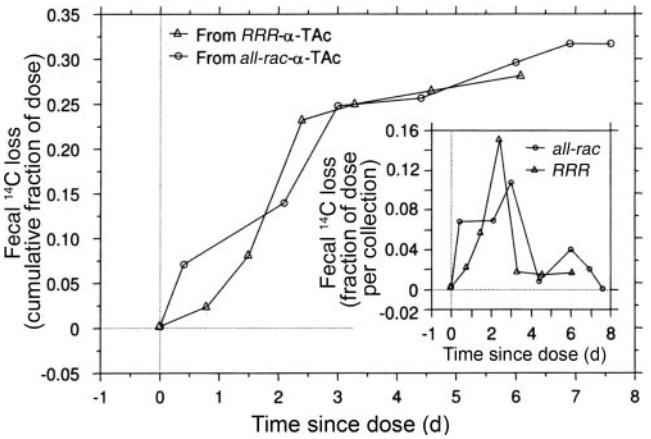

FIGURE 3. Fecal loss of administered ^{14}C by time since dose. Results are shown as the fraction of the ^{14}C dose per collection (inset) and as a cumulative fraction of the dose for both isomers. TAc, tocopheryl acetate.

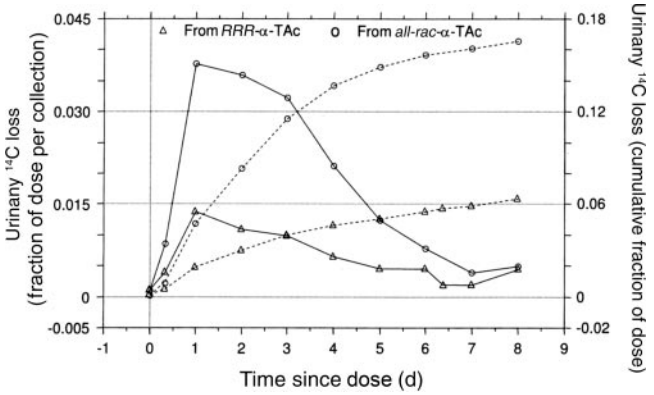

FIGURE 4. Urinary loss of ^{14}C by time since dose. Results are shown as the fraction of the ^{14}C dose per collection (—) and as the cumulative fraction of the dose (- - -) for both isomers. TAc, tocopheryl acetate.

$f(25,7)]]/f(3,1) = [12 - (3.6 - 0.90)]/12$ was 77.5% (44). So the observed tracer data (Figure 3) and model-derived tracee data matched exactly. The chemical identification of the ^{14}C-labeled material in feces was not determined.

The elimination of the ^{14}C tracer in urine is summarized in **Figure 4**. The tracer appeared in urine collected during the first 8 h after dosing and peaked in urine collected between 8 and 24 h. The fraction of the dose eliminated in urine was greater from administered [^{14}C]*all-rac*-α-TAc than from administered [^{14}C]*RRR*-α-TAc, but this difference had disappeared by day 8.

The radiolabeled metabolite in urine is identified as [^{14}C]α-CEHC on the basis of its coelution (on HPLC) with authentic α-CEHC, as shown in **Figure 5**. The top panel shows the third urine collection after dosing; both of these urine samples were treated with glucuronidase. The bottom panel shows the fourth urine collection, when only *all-rac*-TAc isomer was given. This urine sample was analyzed both before and after treatment with glucuronidase to confirm the release of [^{14}C]-α-CEHC. The non-hydrolyzed urine sample also shows a small ^{14}C peak that eluted at ≈11 min. We hypothesized that the small peak of ^{14}C may well be 2,5,7,8-tetramethyl-2(4′-carboxypentyl)-6-hydroxychroman (α-CPHC), the direct precursor of α-CEHC (45).

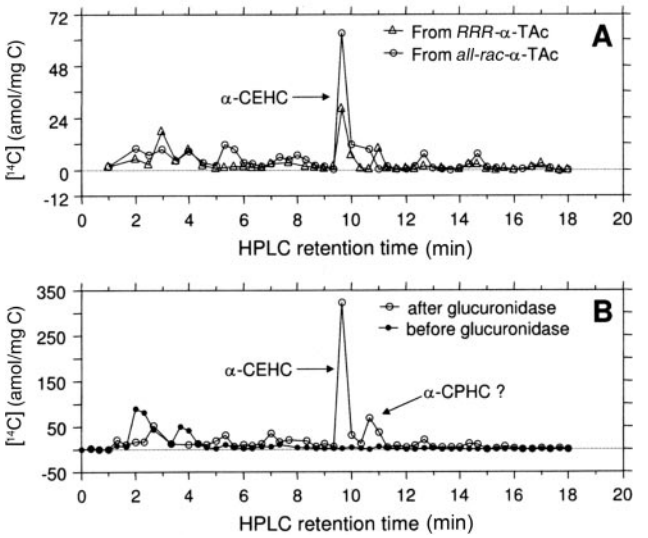

FIGURE 5. HPLC profile of urinary excretion of [^{14}C]α-2,7,8-trimethyl-2-(2-carboxyethyl)-6-hydroxychroman (α-CEHC) identified by its coelution with authentic α-CEHC. A: Third urine collection after dosing; both of these urine samples were treated with glucuronidase. B: Fourth urine collection, when only *all-rac*-tocopheryl acetate (TAc) isomer was given; this urine sample was analyzed both before and after treatment with glucuronidase to confirm the release of [^{14}C]α-CEHC. α-CPHC, 2,5,7,8-tetramethyl-2(4′-carboxypentyl)-6-hydroxychroman; the "?" following "α-CPHC" indicates that the authors hypothesized that the small peak of ^{14}C may well be α-CPHC.

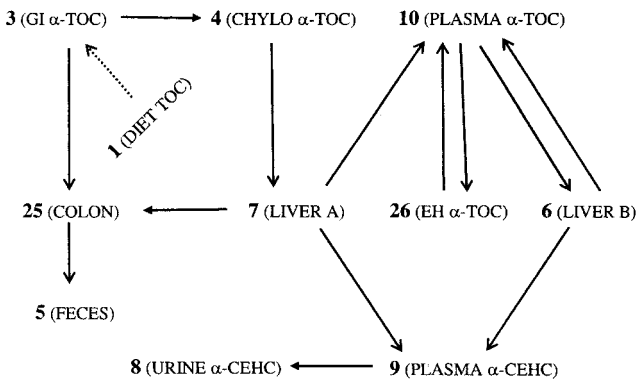

FIGURE 6. In this final model, numbers represent kinetically distinct pools, tentatively identified in parentheses. GI, gastrointestine; TOC, tocopherol; CHYLO, chylomicron; EH, extrahepatic; α-CEHC, [^{14}C]α-2,7,8-trimethyl-2-(2-carboxyethyl)-6-hydroxychroman. Each vector represents material transfer to a recipient from a donor pool. The initial model had kinetic pools of *RRR*-α-tocopherol in gastrointestine, plasma, tissues, feces, and urine. The final model had a delay $d(3,1)$ and 11 kinetically distinct pools. It had 13 rate constants [$k(4,3)$, $k(25,3)$, $k(7,4)$, $k(10,7)$, $k(5,25)$, $k(10,26)$, $k(10,6)$, $k(8,9)$, $k(26,10)$, $k(6,10)$, $k(9,6)$, $k(9,7)$, and $k(25,7)$]; only the last 5 were isomer specific. The sizes of pools 6, 7, 9, 10, 25, and 26 were isomer specific. Tracer and tracee patterns used for parameter estimates and pathways were assumed to be first order.

The final model that was tested and found to be consistent with the full range of our experimental data is shown in **Figure 6**. The numbers represent kinetically distinct pools of α-tocopherol or its metabolites (if identified). The vectors represent material transfer (ie, flow) from a donor pool to a recipient pool. The final model included 11 kinetically distinct pools, which were numbered 1–26 and tentatively identified anatomically in parentheses. Six of the 11 pools (ie, 6, 7, 9, 10, 25, and 26) were isomer-specific. The final model included 13 rate constants, k(to recipient pool i, from donor pool j), of which 5—$k(26,10)$, $k(6,10)$, $k(9,6)$, $k(9,7)$, and $k(25,7)$—were isomer specific.

The plasma, feces, and urine data sets along with the model-fitted lines (model solutions) are shown in **Figure 7**. The lines are functions of model state variables and parameters that were mapped to the experimental data for direct comparison. Log scaling of the ordinate in Figure 7A enabled the plasma kinetic data to be examined closely. The model-fitted lines shown in Figure 7 indicate how well the model fitted the observed data. In Figure 7, model solutions for the plasma (A) and elimination (B) data were excellent, and therefore we accepted the alternate hypothesis (H_a = 2 pools) that 2 functionally distinct pools of α-tocopherol exist in liver—liver A and liver B (Figure 6). The plasma ^{14}C concentrations were higher from administered *RRR*-α-TAc than from *all-rac*-α-TAc. The elimination of ^{14}C from *RRR*-α-TAc and *all-rac*-α-TAc via feces was indistinguishable, which shows that the absorption of the isomers was identical. Elimination of [^{14}C]-α-CEHC via urine was greater from [^{14}C]*all-rac*-α-TAc than from [^{14}C]*RRR*-α-TAc. This greater elimination could also be due to the shorter mean residence times

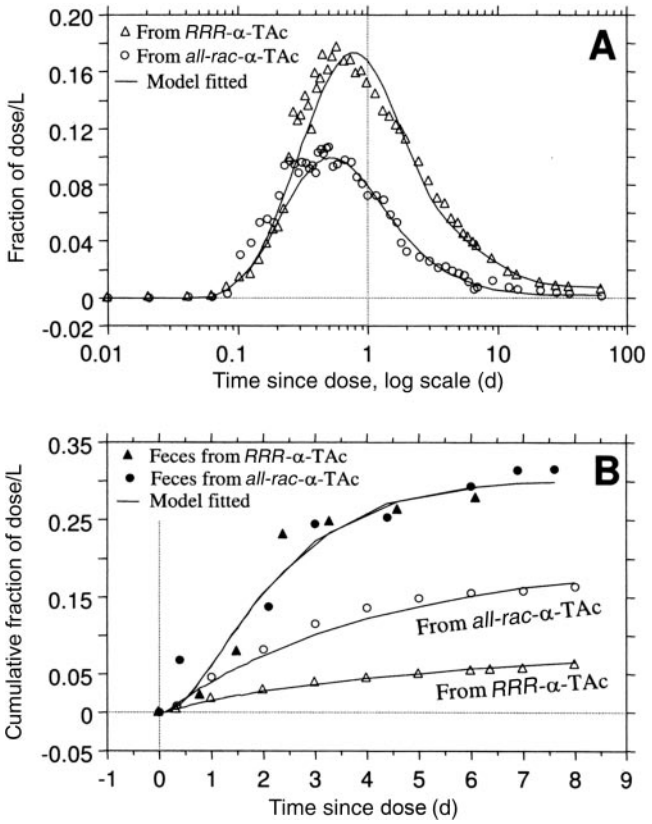

FIGURE 7. Observed data and the lines that were fitted to those data by using the model shown in Figure 6. A: plasma; B: feces and urine (open symbols). The lines are functions of model state variables and parameters that were mapped to the experimental data for direct comparison. TAc, tocopheryl acetate.

of *all-rac*-α-TAc than of *RRR*-α-TAc in most pools, which would favor a more rapid elimination from administered [^{14}C]*all-rac*-α-TAc than from [^{14}C]*RRR*-α-TAc. Had we collected urine over a longer period, the cumulative elimination from both isomers should eventually match. This possibility needs testing.

Furthermore, we considered a liver A delay to better fit the model. A delay can speed up movement to chylomicra tocopherol from gastrointestinal tocopherol and can slightly improve the early upswing fit, especially for the [^{14}C]*all-rac*-tocopherol over *RRR*-α-tocopherol. However, the upswings for [^{14}C]*all-rac*- versus [^{14}C]*RRR*-α-tocopherol were not well separated, and thus a delay did not improve identification of the new parameters because we tried to satisfy minimal difference and maximum simplicity.

The model-estimated daily rate constants of the ^{14}C tracer are summarized in **Table 1**. The constant (k) that described the disposition of the [^{14}C]α-TAc ranged from $k = 0.013$ for $k(10,26)$ to $k = 84.033$ for $k(7,4)$. The fractional SD (FSD) values ranged from 0.038 to 0.226, which indicated good statistical certainty, so that a substantial deterioration of curve fit would follow small changes in rate constants. Five rate constants were smaller for *RRR*-α-tocopherol than for *all-rac*-α-tocopherol. The largest difference between the isomers—$k(9,6)$—was 3.7-fold, whereas the smallest difference—$k(25,7)$—was only 1.08-fold. Eight rate constants were the same for the 2 isomers.

TABLE 1
Model-estimated steady-state daily rate constants for disposition of an oral tracer dose of [^{14}C]*RRR*- and [^{14}C]*all-rac*-α-tocopheryl acetate in a crossover study design[1]

	Formula	k[2]	FSD
Rate constants from *RRR* dose			
To EH α-tocopherol from plasma α-tocopherol	$k(26,10)$	0.863	0.039
To liver kinetic pool B from plasma α-tocopherol	$k(6,10)$	1.484	0.088
To plasma α-CEHC from liver kinetic pool B	$k(9,6)$	0.027	0.095
To plasma α-CEHC from liver kinetic pool A	$k(9,7)$	0.781	0.189
To colon from liver kinetic pool A	$k(25,7)$	2.537	0.226
Rate constants from *all-rac* dose			
To EH α-tocopherol from plasma-α-tocopherol	$k(26,10)$	2.155	0.038
To liver kinetic pool B from plasma α-tocopherol	$k(6,10)$	3.006	0.081
To plasma α-CEHC from liver kinetic pool B	$k(9,6)$	0.099	0.086
To plasma α-CEHC from liver kinetic pool A	$k(9,7)$	1.903	0.193
To colon from liver kinetic pool A	$k(25,7)$	2.752	0.195
Rate constants same from *RRR* and *all-rac* doses			
To chylomicra from gastrointestine	$k(4,3)$	0.841	0.047
To colon from gastrointestine	$k(25,3)$	0.244	0.047
To liver from plasma chylomicra	$k(7,4)$	84.033	0.061
To plasma-α-tocopherol from liver kinetic pool A	$k(10,7)$	22.831	0.161
To feces from colon	$k(5,25)$	0.758	0.111
To plasma-α-tocopherol from EH α-tocopherol	$k(10,26)$	0.013	0.058
To plasma-α-tocopherol from liver kinetic pool B	$k(10,6)$	0.403	0.115
To urine from plasma α-CEHC	$k(8,9)$	46.983	0.130

[1] FSD, SD/mean; EH, extrahepatic; α-CEHC, [^{14}C]α-2, 7, 8-trimethyl-2-(2-carboxyethyl)-6-hydroxychroman.
[2] Rate constants represent the fraction of a donor pool transferred to a recipient pool per day.

The model-estimated steady-state mass distributions and plasma concentrations of tracee for the case of a constant daily α-tocopherol intake (12, 15, or 35 μmol/d) that corresponded to low, intermediate, and RDA (40) for vitamin E are summarized in **Table 2**. The 12 μmol/d intake represents the subject's intake during the study, 35 μmol/d represents the RDA, and 15 μmol/d represents about 1/2 the RDA. These 3 vitamin E intakes were used for simulation. The largest distributions were in pools 10, 26, and 6. Respective distributions in pools 10, 26, and 6 were 6.77, 2.71, and 3.91 times as great for *RRR*-α-tocopherol than for *all-rac*-α-tocopherol. Distributions in all remaining pools (pools 3, 4, 7, 25, and 9) were the same for the 2 isomers. Because the model was composed of linear equations, all distributions increased linearly with intake.

Concentrations of α-tocopherol (the tracee) were 6.5 times as high for *RRR*-α-tocopherol than for *all-rac*-α-tocopherol. Finally, the plasma α-tocopherol concentrations increased linearly with increasing intake, to 31 and 73 μmol/L at α-tocopherol intakes of 15 and 35 μmol/d, respectively. The plasma α-tocopherol concentration of 73 μmol/L was higher than prior

TABLE 2
Model-estimated steady-state α-tocopherol tracee distributions and concentrations in plasma at 3 dietary intakes[1]

		Intake					
		12 μmol/d		15 μmol/d		35 μmol/d	
	Pool	*RRR-*	*all-rac-*	*RRR-*	*all-rac-*	*RRR-*	*all-rac-*
Different for each isomer							
Plasma α-tocopherol	10	88.359	13.035	110.449	16.294	257.713	38.020
EH α-tocopherol	26	5697.04	2098.39	7121.30	2622.99	16 616.40	6120.31
Liver kinetic pool B	6	305.26	78.076	381.58	97.598	890.34	227.71
Same for each isomer							
Gastrointestine	3	11.061	11.061	13.827	13.827	32.262	32.262
Chylomicra	4	0.111	0.111	0.138	0.138	0.323	0.323
Liver kinetic pool A	7	0.338	0.356	0.4229	0.4446	0.9869	1.0374
Colon	25	4.789	4.751	5.987	5.939	13.969	13.858
Plasma α-CEHC	9	0.1781	0.1787	0.2227	0.2234	0.5195	0.5213
Total-body tocopherol mass		6107.12	2205.97	7633.91	2757.48	17 812.43	6434.11
Plasma α-tocopherol tracee (μmol/L)[2]		25	3.7	31	4.6	73	10.8

[1] EH, extrahepatic; α-CEHC, [^{14}C]α-2, 7, 8-trimethyl-2-(2-carboxyethyl)-6-hydroxychroman. Distributions are α-tocopherol tracee, μmol/pool. The 12 μmol/d intake represents the subject's intake during the study, 35 μmol/d represents the Recommended Dietary Allowance, and 15 μmol/d represents approximately one-half the Recommended Dietary Allowance. These 3 vitamin E intakes were used for simulation.
[2] Plasma α-tocopherol tracee is plasma pool/plasma volume (3.53 L).

estimates (46, 47). The mechanisms that limit the rise in plasma α-tocopherol may be triggered at concentrations of ≈25 μmol/L.

Calculated ratios of selected rate constants for the ^{14}C tracer in addition to their ratio of *RRR* to *all-rac* (*RRR:all-rac*), ranked low to high, are shown in the right column in **Table 3**. The ratios indicate the proportions to various pools. The most striking differences were the *RRR:all-rac* of 0.3141 and 0.4321 for low fractional transfers of the *RRR* isomer from Liver A and liver B, respectively, to plasma α-CEHC (a catabolite), which indicated preferential degradation of the *all-rac* isomer by the ω-hydroxylase and elimination via urine. Extrahepatic tissue α-tocopherol had the longest residence time (74.6 d), and it was the same for the *RRR* and *all-rac* isomers. The mean residence times of [^{14}C]*RRR*-α-tocopherol in liver B and plasma were longer than those of [^{14}C]*all-rac*-α-tocopherol in the same tissues. Plasma α-tocopherol had the shortest mean residence time, which was twice as long for the *RRR* as for the *all-rac* isomer.

The calculated daily flows at 3 levels of tracee intake and the flow *RRR:all-rac* (ranked low to high) are shown in **Table 4**. Highest flows were to liver B from plasma α-tocopherol and to plasma α-tocopherol from liver B. When the dietary tracee intake was 35 μmol/d, of the 382.5 μmol *RRR*-α-tocopherol/d that flowed to liver B from plasma α-tocopherol, 358.8 μmol/d (or 93.8%) returned to plasma α-tocopherol, whereas, of the 114.3 μmol *all-rac* isomer/d that flowed to liver B from plasma α-tocopherol, only 91.8 μmol/d (only 80.3%) returned to plasma α-tocopherol. The remaining 23.68 μmol *RRR*-α-tocopherol/d (only 6.19%) flowed to plasma α-CEHC, whereas 22.53 μmol

TABLE 3
Calculated ratios of steady-state rate constants and mean residence times of tracer[1]

		Stereoisomer		
	Calculation	*RRR-*	*all-rac-*	*RRR:all-rac*
Different for each isomer				
To plasma α-CEHC from liver kinetic pool B	$k(9,6)/[k(9,6) + k(10,6)]$	0.0619	0.1971	0.3141
To plasma α-CEHC from liver kinetic pool A	$k(9,7)/[k(9,7) + k(10,7) + k(25,7)]$	0.0299	0.0692	0.4321
To EH α-tocopherol from plasma α-tocopherol	$k(26,10)/[k(26,10) + k(6,10)]$	0.3677	0.4176	0.8805
To colon from liver kinetic pool A	$k(25,7)/[k(25,7) + k(9,7) + k(10,7)]$	0.0970	0.1001	0.9690
To plasma α-tocopherol from liver kinetic pool A	$k(10,7)/[k(10,7) + k(9,7) + k(25,7)]$	0.8731	0.8306	1.0512
To liver kinetic pool B from plasma α-tocopherol	$k(6,10)/[k(6,10) + k(26,10)]$	0.6323	0.5825	1.0855
To plasma α-tocopherol from liver kinetic pool B	$k(10,6)/[k(10,6) + k(9,6)]$	0.9381	0.8029	1.1683
Same for each isomer				
Gastrointestinal absorption (fractional absorption)	$k(4,3)/[k(4,3) + k(25,3)]$	0.775	0.775	1.0000
Mean residence times (d)				
EH α-tocopherol	$1/[k(10,26)]$	74.6269	74.6269	1.0000
Liver kinetic pool A	$1/[k(10,7) + k(9,7) + k(25,7)]$	0.0382	0.0364	1.0494
Liver kinetic pool B	$1/[k(9,6) + k(10,6)]$	2.3277	1.9920	1.1685
Plasma α-tocopherol	$1/[k(26,10) + k(6,10)]$	0.4261	0.1938	2.1986

[1] α-CEHC, [^{14}C]α-2, 7, 8-trimethyl-2-(2-carboxyethyl)-6-hydroxychroman; EH, extrahepatic.

TABLE 4
Calculated flows of α-tocopherol tracee at 3 intakes and the flow ratio *of RRR* to *all-rac* (low to high)[1]

		α-Tocopherol intakes						
		12 μmol/d		15 μmol/d		35 μmol/d		Flow ratio
	Calculation	*RRR-*	*all-rac-*	*RRR-*	*all-rac-*	*RRR-*	*all-rac-*	*RRR:all-rac-*
Different for each isomer								
To plasma α-CEHC from liver kinetic pool A	*f*(9,7)	0.287	0.644	0.347	0.805	0.810	1.878	0.431
To liver kinetic pool B from plasma α-tocopherol	*f*(6,10) = *f*(10,6) + *f*(9,6)[2]	131.1	39.2	163.9	49.0	382.5	114.3	3.346
To plasma α-tocopherol from liver kinetic pool B	*f*(10,6)	123.0	31.5	153.8	39.3	358.8	91.8	3.908
To EH α-tocopherol from plasma α-tocopherol and vice versa	*f*(26,10) = *f*(10,26)[3]	76.3	28.1	95.3	35.1	222.4	81.9	2.715
Same for each isomer								
To chylomicra from gastrointestine and to liver kinetic pool A from chylomicra	*f*(4,3) = *f*(7,4)[3]	9.3	9.3	11.6	11.6	27.1	27.1	1.000
To colon from gastrointestine	*f*(25,3)	2.7	2.7	3.38	3.38	7.88	7.88	1.000
To urine from plasma α-CEHC	*f*(8,9)	8.40	8.37	10.50	10.46	24.49	24.41	1.000
To feces from colon	*f*(5,25)	3.60	3.63	4.50	4.54	10.51	10.59	0.992
To colon from liver kinetic pool A	*f*(25,7)	0.90	0.93	1.13	1.16	2.63	2.72	0.967
To plasma α-tocopherol from liver kinetic pool A and to plasma α-CEHC from liver kinetic pool B	*f*(10,7) = *f*(9,6)[4]	8.12	7.73	10.15	9.66	23.68	22.53	1.051

[1] α-CEHC, [^{14}C]α-2, 7, 8-trimethyl-2-(2-carboxyethyl)-6-hydroxychroman; EH, extrahepatic. Tracee mass-transferred to recipient from donor pools in μmol/d.

[2] At 35 μmol/d intake, 94% (358.8/382.5) of *RRR*-α-tocopherol flowing to liver α-tocopherol from plasma α-tocopherol returned to plasma tocopherol, but only 80% (91.8/114.3) of *all-rac*-α-tocopherol did so; the remainder flowed to plasma α-CEHC and urine.

[3] All tracee (both isomers) delivered to chylomicra went to liver kinetic pool A. All tracee (both isomers) flowing to EH α-tocopherol returned to plasma α-tocopherol.

[4] All tracee flowing to plasma α-tocopherol from liver kinetic pool A flowed to plasma α-CEHC and eventually to urine. The 12 μmol/d Intake represents the subject's intake during the study, 35 μmol/d represents the Recommended Dietary Allowance, and 15 μmol/d represents approximately one-half the Recommended Dietary Allowance. The 3 vitamin E intakes were used for simulation.

all-rac-α-tocopherol/d (or 19.7%) did so. The flow to plasma α-CEHC from liver A was only 0.81 μmol/d for the *RRR* isomer but 1.878 μmol/d for the *all-rac* isomer, for *RRR:all-rac* of 0.431, which suggests that the *all-rac* isomer was preferentially degraded and eliminated as α-CEHC in urine.

DISCUSSION

Despite its nutritional importance, quantitation of human vitamin E metabolism is incomplete (3–5). Therefore, we conducted a crossover feasibility study and kinetically modeled the data set to quantify the behavior of *RRR*- and *all-rac*-α-tocopherol in a healthy man. We first followed the fate of administered [5-^{14}CH$_3$]*RRR*-α-TAc in the subject's plasma, plasma lipoproteins, urine, and feces over time. After a 3-mo washout period, we repeated the study with [5-^{14}CH$_3$]*all-rac*-α-TAc. The subject's dietary α-tocopherol intake was 12 ± 4 μmol/d, and his plasma α-tocopherol at 22.9 ± 1 μmol/L was below the threshold (30 μmol/L) for α-CEHC transfer into urine (42).

The ^{14}C tracer profiles in plasma (Figure 1), feces (Figure 3), and urine (Figure 4) were consistent with prior estimates (7, 48). ^{14}C tracer profiles in plasma lipoproteins (Figure 2) also were consistent with previous reports (49–53), and HDL had a low concentration of the ^{14}C tracer, which reflects the key donor role for vitamin E (54, 55). Others already showed that the mechanisms of degradation and elimination were the same for all forms of tocopherol (42, 56), but the rates were higher for γ-tocopherol than for α-tocopherol (57). Others also showed that the *all-rac*-α-tocopherol isomer was preferentially degraded to α-CEHC over the *RRR*-α-tocopherol isomer (37, 58); our 3-fold elimination of the ^{14}C tracer in urine in Figure 4 was consistent with the earlier findings. Finally, our confirmation of [^{14}C]α-CEHC as a key (but not the only) metabolite of α-tocopherol in urine (Figure 5) fit well with prior reports (1, 2, 13, 17, 22, 42, 57, 59, 60). Therefore, our feasibility study yielded a data set that matched prior estimates well and that was suitable for kinetic modeling.

We built a kinetic model (Figure 6) to obtain values for critical parameters of the model and to identify unique and testable hypotheses about α-tocopherol metabolism. α-Tocopherol transfer protein not only catalyzes the intermembrane transfer of α-tocopherol to recipient from donor membranes (61, 62) but also retains and secretes α-tocopherol from hepatocytes to circulating lipoproteins for delivery to extrahepatic tissues (63–66). In addition, [^{14}C]α-tocopheryl phosphate (TP, a new, natural form of α-tocopherol) was discovered in the liver of a rat given an oral dose of [^{14}C]α-tocopherol (8). If the intermembrane transfer, the secretion, and the existence of TP were independent features (which is still not known), it would mean that liver had more than one distinct kinetic pool of α-tocopherol. Therefore, we tested the hypothesis that liver had 2 kinetic pools of α-tocopherol, ie, liver A and liver B (H_o = 1 pool against H_a = 2 pools). We used a paired *t* test of the difference between the observed plasma data minus the 2-pool-model solution for it and

the observed plasma data minus the 1-pool-model solution for it. That mean (±SE) difference, −0.005652 ± 0.001374 ($n = 108$), was significant ($P < 0.0001$), which showed the existence of 2 kinetically distinct pools in liver. Thus, with 2 distinct kinetic pools in liver, a delay $d(3,1)$, and a renal clearance for plasma α-CEHC, the final model (Figure 6) fit the very informative plasma, feces, and urine ^{14}C data extremely well (Figure 7). We tentatively identified the pools as liver A and liver B.

The tracee distributions rose as α-tocopherol intake increased, and they rose more for *RRR*- than for *all-rac*-α-tocopherol (Table 2). The distributions and their relation to rising intake were consistent with the greater enrichment of mouse plasma (and tissues) with hexadeuterated *RRR*-α-tocopherol than with the trideuterated *all-rac*-α-tocopherol in mice (67). The tracee distributions also matched prior estimates of 6700 ± 860 μmol (68) and 2000–26000 μmol (69) in adipose tissue, a major store.

The only exception was the poor match to a physiological level for the plasma α-tocopherol; the model estimated 31 and 73 μmol/L for *RRR*-α-tocopherol intakes of 15 and 35 μmol/d, respectively. The 73 μmol/L concentration was higher than expected (46, 47), which suggested that the kinetics of α-tocopherol became nonlinear between intakes of 15 and 35 μmol/d. Because kinetic models enable plasma α-tocopherol concentrations to be simulated for varied intakes, we performed additional simulations to bring plasma α-tocopherol more in line with the prior estimate of ≈28 μmol/L for an *RRR*-α-tocopherol intake of 35 μmol/d. First**,** we increased the flow [$f(8,9)$]; this step did not lower plasma *RRR*-α-tocopherol concentrations, which indicated that formation rather than elimination of α-CEHC has a rate-limiting effect. Second**,** we reduced fractional absorption, $k(4,3)/(k(4,3)+k(25,3)$, from 0.775 to 0.30; this step reduced the plasma α-tocopherol to 28 μmol/L, but the 0.30 value was inconsistent with prior estimates (7, 48). Third**,** we raised $k(9,7)$ from 0.781 to 39.0, and that step reduced the plasma α-tocopherol to 29 μmol/L. Fourth**,** we raised $k(9,6)$ from 0.027 to 0.081, and that step reduced plasma α-tocopherol to 27 μmol/L. Only the third and fourth simulations were effective, which indicates that they are rate-limiting pathways. The performance of the 4 additional stimulations shows how dose-response tracer modeling can identify control pathways.

In Table 3, the highest *RRR*:*all-rac* of 1.1683 showed a greater recycling of the *RRR* isomer to the plasma (70–73) from liver B (61, 67). In contrast, *all-rac*-tocopherol was preferentially degraded to plasma α-CEHC (0.1971 over 0.0619 and 0.0692 over 0.0299), to colon (0.1001 over 0.0970), and to extrahepatic tissue (0.4176 over 0.3677). The most striking difference was the rate-constant *RRR*:*all-rac* of 0.3141 and 0.4321 (Table 3) for high fractional transfers of the *all-rac* isomer from liver B to plasma α-CEHC. Thus, we quantified the degradation of the *all-rac* over the *RRR* isomer α-CEHC (74), and we do not support a trigger threshold for α-CEHC elimination (42) because [^{14}C]α-CEHC was formed and eliminated well below the RDA intake of α-tocopherol.

It is important to note that, although tracer rate constant $k(26,10)$ in Table 1 was smaller for *RRR*-α-tocopherol (0.863 ± 0.039) than for *all-rac*-α-tocopherol (2.155 ± 0.038), tracee flows $f(26,10)$ in Table 4 were larger for *RRR*-α-tocopherol (76.3 μmol/d) than for *all-rac*-α-tocopherol (28.1 μmol/d). This occurred because of a larger tracee distribution of *RRR*-α-tocopherol (88.359 μmol) than of *all-rac*-α-tocopherol (13.035 μmol) (Table 2). The same happened with urine (Tables 2 and 3). The larger distributions of *RRR*-α-tocopherol than of *all-rac*-α-tocopherol in pools 26 (5697 > 2098 μmol) and 6 (305 > 78 μmol) (Table 2), coupled with the smaller *RRR*:*all-rac* to plasma α-CEHC from liver B (0.3141) and liver A (0.4321) (Table 3), account for the greater amount of ^{14}C tracer from *all-rac*-α-tocopherol than from *RRR*-α-tocopherol in urine. Furthermore, with an intake of 12 μmol/d, the *RRR*-α-tocopherol distribution in liver B was ≈4 times that of *all-rac*-α-tocopherol. The proportion of tracee flowing from liver B to plasma α-CEHC for *all-rac*-α-tocopherol was ≈3.2 times that for *RRR*-α-tocopherol, and thus the *RRR*-α-tocopherol ^{14}C tracer experienced a greater dilution than did *all-rac*-α-tocopherol ^{14}C tracer with the tracee. Consequently, less *RRR*-α-tocopherol ^{14}C tracer than *all-rac* entered plasma α-CEHC, which forced the ^{14}C tracer mass in urine to be greater for *all-rac*-α-tocopherol. It is important to notice that the tracee flows to urine were similar for the 2 isomers. This finding shows how the kinetic modeling of tracer data sets can explain or reconcile tracer and tracee data that may appear as conflicting steady-state flows.

In conclusion, we quantified the absorption, distribution, metabolism, and elimination of a true tracer dose of [^{14}C]*RRR*-α-tocopherol in a healthy man under steady-state conditions and quantified α-tocopherol metabolism as it might occur in vivo. We found that liver has 2 kinetically distinct α-tocopherol pools, that α-CEHC is eliminated in urine in the absence of vitamin E supplementation, and that *all-rac*-α-tocopherol is preferentially degraded and eliminated in urine. Our approach, data set, and model-derived features of human vitamin E metabolism encourage further testing.

We thank Willy Cohn for his valuable input and discussions in designing the study, developing the model, and interpreting the results; John Vogel, Ted Ognibene, Bruce Buchholz, and Kurt Haack for the ^{14}C measurements; and *AJCN* reviewers for their perceptive and helpful comments.

AJC designed the study and wrote the manuscript; FFM, CCH, and JCC participated in the sample preparation and analyses; JF participated in the diet analyses; JAN, JGF, and AJC developed the model and interpreted the results. None of the authors had a personal or financial conflict of interest.

REFERENCES

1. Ferslew KE, Acuff RV, Daigneault EA, Woolley TW, Stanton PE Jr. Pharmacokinetics and bioavailability of the RRR and all racemic stereoisomers of alpha-tocopherol in humans after single oral administration. J Clin Pharmacol 1993;33:84–8.
2. Burton GW, Traber MG, Acuff RV, et al. Human plasma and tissue alpha-tocopherol concentrations in response to supplementation with deuterated natural and synthetic vitamin E. Am J Clin Nutr 1998;67:669–84.
3. Cohn W. Evaluation of vitamin E potency. Am J Clin Nutr 1999;69:156–8.
4. Hoppe PP, Krennrich G. Bioavailability and potency of natural-source and all-racemic alpha-tocopherol in the human: a dispute. Eur J Nutr 2000;39:183–93.
5. Blatt DH, Pryor WA, Mata JE, Rodriguez-Proteau R. Re-evaluation of the relative potency of synthetic and natural alpha-tocopherol: experimental and clinical observations. J Nutr Biochem 2004;15:380–95.
6. Blomstrand R, Forsgren L. Labelled tocopherols in man. Intestinal absorption and thoracic-duct lymph transport of dl-alpha-tocopheryl-3,4–14C2 acetate dl-alpha-tocopheramine-3,4–14C2 dl-alpha-tocopherol-(5-methyl-3H) and N-(methyl-3H)-dl-gamma-tocopheramine. Int Z Vitaminforsch 1968;38:328–44.
7. Mac Mahon MT, Neale G. The absorption of alpha-tocopherol in control subjects and in patients with intestinal malabsorption. Clin Sci 1970;38:197–210.
8. Gianello R, Libinaki R, Azzi A, et al. Alpha-tocopheryl phosphate: a novel, natural form of vitamin E. Free Radic Biol Med 2005;39:970–6.

9. Burton GW, Ingold KU, Foster DO, et al. Comparison of free alpha-tocopherol and alpha-tocopheryl acetate as sources of vitamin E in rats and humans. Lipids 1988;23:834–40.
10. Cheeseman KH, Holley AE, Kelly FJ, Wasil M, Hughes L, Burton G. Biokinetics in humans of RRR-alpha-tocopherol: the free phenol, acetate ester, and succinate ester forms of vitamin E. Free Radic Biol Med 1995;19:591–8.
11. Ingold KU, Burton GW, Foster DO, Hughes L, Lindsay DA, Webb A. Biokinetics of and discrimination between dietary RRR- and SRR-alpha-tocopherols in the male rat. Lipids 1987;22:163–72.
12. Burton GW, Ingold KU, Cheeseman KH, Slater TF. Application of deuterated alpha-tocopherols to the biokinetics and bioavailability of vitamin E. Free Radic Res Commun 1990;11:99–107.
13. Traber MG, Ramakrishnan R, Kayden HJ. Human plasma vitamin E kinetics demonstrate rapid recycling of plasma RRR-alpha-tocopherol. Proc Natl Acad Sci U S A 1994;91:10005–8.
14. Leonard SW, Good CK, Gugger ET, Traber MG. Vitamin E bioavailability from fortified breakfast cereal is greater than that from encapsulated supplements. Am J Clin Nutr 2004;79:86–92.
15. Bruno RS, Leonard SW, Park SI, Zhao Y, Traber MG. Human vitamin E requirements assessed with the use of apples fortified with deuterium-labeled alpha-tocopheryl acetate. Am J Clin Nutr 2006;83:299–304.
16. Burton GW, Ingold KU, Traber MG, Kayden H. Reply to W Cohn. Am J Clin Nutr 1999;69:157–58 (letter).
17. Acuff RV, Thedford SS, Hidiroglou NN, Papas AM, Odom TA Jr. Relative bioavailability of *RRR*- and *all-rac*-alpha-tocopheryl acetate in humans: studies using deuterated compounds. Am J Clin Nutr 1994;60:397–402.
18. Sowell AL, Huff DL, Yeager PR, Caudill SP, Gunter EW. Retinol, alpha-tocopherol, lutein/zeaxanthin, beta-cryptoxanthin, lycopene, alpha-carotene, trans-beta-carotene, and four retinyl esters in serum determined simultaneously by reversed-phase HPLC with multiwavelength detection. Clin Chem 1994;40:411–6.
19. Morinobu T, Yoshikawa S, Hamamura K, Tamai H. Measurement of vitamin E metabolites by high-performance liquid chromatography during high-dose administration of alpha-tocopherol. Eur J Clin Nutr 2003;57:410–4.
20. Vogel JS. Rapid production of graphite without contamination for biomedical AMS. Radiocarbon 1992;34:344–50.
21. Ognibene TJ, Bench G, Vogel JS, Peaslee GF, Murov S. A high-throughput method for the conversion of CO2 obtained from biochemical samples to graphite in septa-sealed vials for quantification of 14C via accelerator mass spectrometry. Anal Chem 2003;75:2192–6.
22. Pope SA, Clayton PT, Muller DP. A new method for the analysis of urinary vitamin E metabolites and the tentative identification of a novel group of compounds. Arch Biochem Biophys 2000;381:8–15.
23. Vogel JS, Turteltaub KW, Finkel R, Nelson DE. Accelerator mass spectrometry. Anal Chem 1995;67:353A–9A.
24. Bjorneboe A, Bjorneboe GE, Drevon CA. Absorption, transport and distribution of vitamin E. J Nutr 1990;120:233–42.
25. Parker RS, Swanson JE, You CS, Edwards AJ, Huang T. Bioavailability of carotenoids in human subjects. Proc Nutr Soc 1999;58:155–62.
26. Huuskonen J, Olkkonen VM, Jauhiainen M, Ehnholm C. The impact of phospholipid transfer protein (PLTP) on HDL metabolism. Atherosclerosis 2001;155:269–81.
27. Kaempf-Rotzoll DE, Traber MG, Arai H. Vitamin E and transfer proteins. Curr Opin Lipidol 2003;14:249–54.
28. Porter TD. Supernatant protein factor and tocopherol-associated protein: an unexpected link between cholesterol synthesis and vitamin E. J Nutr Biochem 2003;14:3–6.
29. Mardones P, Rigotti A. Cellular mechanisms of vitamin E uptake: relevance in alpha-tocopherol metabolism and potential implications for disease. J Nutr Biochem 2004;15:252–60.
30. Stocker A. Molecular mechanisms of vitamin e transport. Ann N Y Acad Sci 2004;1031:44–59.
31. Toth PP, Davidson MH. Therapeutic interventions targeted at the augmentation of reverse cholesterol transport. Curr Opin Cardiol 2004;19:374–9.
32. Schneider C. Chemistry and biology of vitamin E. Mol Nutr Food Res 2005;49:7–30.
33. Stefanovski D, Moate PJ, Boston RC. WinSAAM: a Windows-based compartmental modeling system. Metabolism 2003;52:1153–66.
34. Novotny JA, Greif P, Boston RC. WinSAAM: application and explanation of use. Adv Exp Med Biol 2003;537:343–51.
35. Stahl W, Graf P, Brigelius-Flohe R, Wechter W, Sies H. Quantification of the alpha- and gamma-tocopherol metabolites 2,5,7, 8-tetramethyl-2-(2′-carboxyethyl)-6-hydroxychroman and 2,7, 8-trimethyl-2-(2′-carboxyethyl)-6-hydroxychroman in human serum. Anal Biochem 1999;275:254–9.
36. Radosavac D, Graf P, Polidori MC, Sies H, Stahl W. Tocopherol metabolites 2, 5, 7, 8-tetramethyl-2-(2′-carboxyethyl)-6-hydroxychroman (alpha-CEHC) and 2, 7, 8-trimethyl-2-(2′-carboxyethyl)-6-hydroxychroman (gamma-CEHC) in human serum after a single dose of natural vitamin E. Eur J Nutr 2002;41:119–24.
37. Bruno RS, Leonard SW, Li J, Bray TM, Traber MG. Lower plasma alpha-carboxyethyl-hydroxychroman after deuterium-labeled alpha-tocopherol supplementation suggests decreased vitamin E metabolism in smokers. Am J Clin Nutr 2005;81:1052–9.
38. Yoshikawa S, Morinobu T, Hamamura K, Hirahara F, Iwamoto T, Tamai H. The effect of gamma-tocopherol administration on alpha-tocopherol levels and metabolism in humans. Eur J Clin Nutr 2005;59:900–5.
39. Snyder WS, Cook MJ, Karhausen LR, Nasset ES, Howells GP Tipton IH, eds. Report of the Task Group on Reference Man. A report prepared by a task group of Committee 2 of the International Commission on Radiological Protection. ICRP Publication 23. Oxford, United Kingdom: Pergamon Press, 1975.
40. Institute of Medicine. Dietary reference intakes for vitamin C, vitamin E, selenium, and carotenoids. Washington, DC: National Academy Press, 2000.
41. Berman M. A postulate to aid in model building. J Theor Biol 1963;4:229–36.
42. Schultz M, Leist M, Petrzika M, Gassmann B, Brigelius-Flohe R. Novel urinary metabolite of alpha-tocopherol, 2,5,7,8-tetramethyl-2(2′-carboxyethyl)-6-hydroxychroman, as an indicator of an adequate vitamin E supply? Am J Clin Nutr 1995;62(suppl):1527S–34S.
43. Ferrel P. Deficiency states, pharmacological effects, and nutrient requirements. New York, NY: Marcel Dekker Inc, 1980.
44. Clifford AJ. The whole animal as an analytical tool. New York, NY: Marcel Dekker Inc, 1984.
45. Schuelke M, Elsner A, Finckh B, Kohlschutter A, Hubner C, Brigelius-Flohe R. Urinary alpha-tocopherol metabolites in alpha-tocopherol transfer protein-deficient patients. J Lipid Res 2000;41:1543–51.
46. Horwitt MK. Vitamin E and lipid metabolism in man. Am J Clin Nutr 1960;8:451–61.
47. Princen HM, van Duyvenvoorde W, Buytenhek R, et al. Supplementation with low doses of vitamin E protects LDL from lipid peroxidation in men and women. Arterioscler Thromb Vasc Biol 1995;15:325–33.
48. Kelleher J, Losowsky MS. The absorption of alpha-tocopherol in man. Br J Nutr 1970;24:1033–47.
49. Jeanes YM, Hall WL, Lodge JK. Comparative (2)H-labelled alpha-tocopherol biokinetics in plasma, lipoproteins, erythrocytes, platelets and lymphocytes in normolipidaemic males. Br J Nutr 2005;94:92–9.
50. Borel P, Pasquier B, Armand M, et al. Processing of vitamin A and E in the human gastrointestinal tract. Am J Physiol Gastrointest Liver Physiol 2001;280:G95–103.
51. Hall WL, Jeanes YM, Lodge JK. Hyperlipidemic subjects have reduced uptake of newly absorbed vitamin E into their plasma lipoproteins, erythrocytes, platelets, and lymphocytes, as studied by deuterium-labeled alpha-tocopherol biokinetics. J Nutr 2005;135:58–63.
52. Massey JB. Kinetics of transfer of alpha-tocopherol between model and native plasma lipoproteins. Biochim Biophys Acta 1984;793:387–92.
53. Traber MG, Lane JC, Lagmay NR, Kayden HJ. Studies on the transfer of tocopherol between lipoproteins. Lipids 1992;27:657–63.
54. Kolleck I, Schlame M, Fechner H, Looman AC, Wissel H, Rustow B. HDL is the major source of vitamin E for type II pneumocytes. Free Radic Biol Med 1999;27:882–90.
55. Goti D, Hammer A, Galla HJ, Malle E, Sattler W. Uptake of lipoprotein-associated alpha-tocopherol by primary porcine brain capillary endothelial cells. J Neurochem 2000;74:1374–83.
56. Chicku S, Hamamura K, Nakamura T. Novel urinary metabolite of d-d-tocopherol in rats. J Lipid Res 1984;25:40–8.
57. Swanson JE, Ben RN, Burton GW, Parker RS. Urinary excretion of 2,7,8-trimethyl-2-(beta-carboxyethyl)-6-hydroxychroman is a major route of elimination of gamma-tocopherol in humans. J Lipid Res 1999;40:665–71.
58. Traber MG. The biological activity of vitamin E. Corvallis, OR: The Linus Pauling Institute, 1998.

59. Kiyose C, Muramatsu R, Kameyama Y, Ueda T, Igarashi O. Biodiscrimination of alpha-tocopherol stereoisomers in humans after oral administration. Am J Clin Nutr 1997;65:785–9.
60. Sontag TJ, Parker RS. Cytochrome P450 omega-hydroxylase pathway of tocopherol catabolism. Novel mechanism of regulation of vitamin E status. J Biol Chem 2002;277:25290–6.
61. Hosomi A, Arita M, Sato Y, et al. Affinity for alpha-tocopherol transfer protein as a determinant of the biological activities of vitamin E analogs. FEBS Lett 1997;409:105–8.
62. Morley S, Panagabko C, Stocker A, Atkinson J, Manor D. Structure-function relationship in the tocopherol transfer protein. Ann N Y Acad Sci 2004;1031:332–3.
63. Arita M, Nomura K, Arai H, Inoue K. alpha-tocopherol transfer protein stimulates the secretion of alpha-tocopherol from a cultured liver cell line through a brefeldin A-insensitive pathway. Proc Natl Acad Sci U S A 1997;94:12437–41.
64. Horiguchi M, Arita M, Kaempf-Rotzoll DE, Tsujimoto M, Inoue K, Arai H. pH-dependent translocation of alpha-tocopherol transfer protein (alpha-TTP) between hepatic cytosol and late endosomes. Genes Cells 2003;8:789–800.
65. Qian J, Atkinson J, Manor D. Biochemical consequences of heritable mutations in the alpha-tocopherol transfer protein. Biochemistry 2006; 45:8236–42.
66. Qian J, Morley S, Wilson K, Nava P, Atkinson J, Manor D. Intracellular trafficking of vitamin E in hepatocytes: the role of tocopherol transfer protein. J Lipid Res 2005;46:2072–82.
67. Leonard SW, Terasawa Y, Farese RV Jr, Traber MG. Incorporation of deuterated *RRR*- or *all-rac*-alpha-tocopherol in plasma and tissues of alpha-tocopherol transfer protein–null mice. Am J Clin Nutr 2002;75: 555–60.
68. Kayden HJ. Tocopherol content of adipose tissue from vitamin E-deficient humans. Ciba Found Symp 1983;101:70–91.
69. Parker RS. Carotenoid and tocopherol composition of human adipose tissue. Am J Clin Nutr 1988;47:33–6.
70. Traber MG, Burton GW, Ingold KU, Kayden HJ. RRR- and SRR-alpha-tocopherols are secreted without discrimination in human chylomicrons, but RRR-alpha-tocopherol is preferentially secreted in very low density lipoproteins. J Lipid Res 1990;31:675–85.
71. Traber MG, Rudel LL, Burton GW, Hughes L, Ingold KU, Kayden HJ. Nascent VLDL from liver perfusions of cynomolgus monkeys are preferentially enriched in RRR- compared with SRR-alpha-tocopherol: studies using deuterated tocopherols. J Lipid Res 1990;31:687–94.
72. Traber MG, Sokol RJ, Burton GW, et al. Impaired ability of patients with familial isolated vitamin E deficiency to incorporate alpha-tocopherol into lipoproteins secreted by the liver. J Clin Invest 1990;85:397–407.
73. Catignani GL, Bieri JG. Rat liver alpha-tocopherol binding protein. Biochim Biophys Acta 1977;497:349–57.
74. Traber MG, Elsner A, Brigelius-Flohe R. Synthetic as compared with natural vitamin E is preferentially excreted as alpha-CEHC in human urine: studies using deuterated alpha-tocopheryl acetates. FEBS Lett 1998;437:145–8.